

SUPPLEMENTAL INFORMATION

DEAD-box Helicase DP103 Defines Metastatic Potential of Human Breast Cancers

Eun Myoung Shin, Hui Sin Hay, Moon Hee Lee, Jen Nee Goh, Tuan Zea Tan, Yin Ping Sen, See Wee Lim, Einas M. Yousef, Hooi Tin Ong, Aye Aye Thike, Xiangjun Kong, Zhengsheng Wu, Earnest Mendoz, Wei Sun, Manuel Salto-Tellez, Chwee Teck Lim, Peter E. Lobie, Yoon Pin Lim, Celestial T. Yap, Qi Zeng, Gautam Sethi, Martin B. Lee, Patrick Tan, Boon Cher Goh, Lance D. Miller, Jean Paul Thiery, Tao Zhu, Louis Gaboury, Puay Hoon Tan, Kam Man Hui, George Wai-Cheong Yip, Shigeaki Miyamoto, Alan Prem Kumar, Vinay Tergaonkar

SUPPLEMENTAL METHODS

Transfection, siRNA and plasmids

Two unique siRNAs targeting non-conserved coding regions of DP103 were used: #1: 5'-CCAGUGAUCCAAGUCUCAUAGCUUU-3'; #2: 5'-GCUGCCGCUUCUCAU CAUUAUUAUU-3' (Stealth RNAi™, Invitrogen, Life Technologies, Grand Island, NY). 5'-AGC UUC AUA AGG CGC AUG CTT (luciferase gene sequence inverted) was used as control siRNA (Qiagen, Valencia, CA). Full length-hFLAG-DP103 pcDNA3 was cloned from full length 2FLAG-hDP103, a kind gift from C. Glass (26). Helicase-dead mutant 2FLAG-hDP103-GNT pcDNA was derived from 2FLAG-hDP103 pcDNA by PCR-mutagenesis (Stratagene, La Jolla, CA) using sense primer 5'-TCTGGTACCGGGAATACCTGTGTGTTC-3' and antisense primer 5'-GAACACACAGGTATTCCCGGTACCAGA-3. The critical lysine residue needed to bind ATP (GKT) was mutated to an asparagines residue (GNT). For retroviral DP103 plasmid construction, a forward primer containing AgeI site and a reverse primer containing XhoI site was used to amplify the DP103 cDNA from Full length-hFLAG-DP103 pcDNA3. The amplified fragment was cloned into AgeI-XhoI cut pBobi plasmid, which contains a lentiviral backbone with the restriction sites placed immediately downstream of the Flag tag which is preceded by a CMV promoter. The primer sequences are: sense primer 5'-ATT

AACCGGTATGGACTACAAGGAC-3' and antisense primer 5'-ATTACTCGA
GTCACTGGTTACTATGCATC-3'.

Western Analysis

At the time of harvesting, the cell pellets were collected and completely lysed with RIPA lysis buffer (50mM Tris at pH 7.5, 150mM NaCl, 1% v/v NP-40, 1% v/v deoxycholic acid, 0.1% v/v SDS and 1mM EDTA) containing 1mM PMSF, leupeptin, pepstatin A and aprotinin before subjected to SDS-PAGE. The resolved proteins were then transferred onto nitrocellulose transfer membrane, blocked with 5% milk and incubated with specific primary antibodies at 4°C overnight, followed by secondary antibodies before visualizing on X-ray films using enhanced chemiluminescence (Pierce, Rockford, IL). Human anti-mouse DP103 was purchased from BD Transduction Laboratories (San Diego, CA), human anti-rabbit MMP9, human anti-rabbit p-IkB α (Ser32/Ser36), human anti-rabbit ICAM, goat anti-mouse and goat anti-rabbit from Cell Signaling (Danvers, MA), human anti-rabbit TAK1 (H-579), TAB2 (H-300), TAB3 (H-128), TRF2 (N-20), c-Jun (H-79), NEMO (FL-419), IKK1/2 (H-470), p65 (C-20), p50 (H119), GAPDH (6C5), normal rabbit IgG and anti-mouse Myc (9E10) from Santa Cruz (CA, USA), anti-mouse Flag M2 from Sigma (St Louis, MO), anti-phospho-IKK1/2 (Ser180/181) from bioworld Technology (Louis Park, MN) anti-rat HA from Roche (Indianapolis, IN), and human anti-mouse SUMO-1 from Zymed (South San Francisco, CA).

RNA isolation, reverse transcription and realtime-PCR

Total RNA was extracted using TRIzol® reagent according to the manufacturer's instructions (Invitrogen, Life Technologies, Grand Island, NY). Reverse transcription (RT) was then carried

out. Each RT reaction contains 1µg of total RNA, 1x RT buffer, 5mM MgCl₂, 425µM each of dNTPs, 2µM random hexamers, 0.35U/µl RNase inhibitor, 1.1U/µl MultiScribe reverse transcriptase and made up to 10µl with sterile water. RT reaction was carried out at 42°C for 1h. The relative expressions of various genes were then analyzed using quantitative RT-PCR (ABI PRISM 7500, Applied Biosystems, Foster City, CA, USA) with 18S as an internal control. Primers and probes were purchased as kits from Applied Biosystems (Assays-on-Demand).

Invasion assay

In vitro invasion assay was performed using BD Bio-Coat Matrigel invasion assay system (BD Biosciences, San Jose, CA) according to the manufacturer's instructions. Briefly, cells were trypsinized 48h post-transfection, 2×10^5 cells suspended in serum-free medium and seeded into the Matrigel transwell chambers consisting of polycarbonate membranes with 8-µm pores. After incubation for 24h, the upper surface of transwell chambers was wiped off with a cotton swab and invading cells were fixed and stained with crystal violet solution. The invading cell numbers were counted in five randomly selected microscope fields (x200) and their averages were converted to percentage with the control setup taken to be at 100%.

Immunoprecipitation

A total of 3×10^6 cells were treated as indicated. Cell pellets were lysed in lysis buffer (50mM Tris [pH 7.4], 150mM NaCl, 0.5% NP-40, 0.5mM PMSF, 20mM β-glycerol phosphate, 1mM sodium orthovanadate, 1µg/ml leupeptin, 1µg/ml aprotinin, 50mM sodium fluoride). Pre-cleared 0.5mg of proteins were incubated with Protein A Sepharose, CL-4B (GE Healthcare Life Science, Pittsburgh, PA) and indicated antibodies (1µg) overnight. Beads were washed four times with (200mM Tris [pH 8], 100mM NaCl, 0.5% NP-40, 2mM DTT, 0.5mM PMSF, 1mM sodium

orthovanadate, 1 μ g/ml leupeptin, 1 μ g/ml aprotinin). The samples were boiled in 4x SDS loading buffer, and proteins were separated by SDS-PAGE and subjected to Western blotting with the indicated antibodies.

Wound healing assay

MDA-MB-231 and BT549 cells were treated according to experimental design. Before plating the cells, two parallel lines were drawn at the underside of the well. These lines served as fiducial marks for the wound areas to be analyzed. In preparation for marking the wound, the cells should be fully confluent. The growth medium was aspirated and replaced by calcium-free PBS to prevent killing of cells at the edge of the wound by exposure to high calcium concentrations. Two parallel scratch wounds were made perpendicular to the marker lines with a 1000 μ l blue tip. The medium was then changed to complete media. After incubation for 48h, the wounds are observed using bright field microscopy and multiple images were taken at areas flanking the intersections of the wound and the marker lines at the start and end of the experiment. Three measurements of the gap distance between the wound were taken at the start and end of the experiment from the images, and their averages are converted to percentages to depict percentage change with the control setup taken to be at 100%.

Electrophoretic mobility shift assay

Cell pellets were lysed in Totex buffer (20mM HEPES [pH 7.7], 350mM NaCl, 20% glycerol, 1% NP-40, 1mM MgCl₂, 0.5mM EDTA, 0.1mM EGTA, 0.5mM DTT) containing protease inhibitors, spun down at 14,000 x *g* for 10min at 4°C and subjected to EMSA as described previously (114). The supernatant collected was divided into three separate samples for analysis

with double-stranded NFκB, AP-1 and Oct-1 [γ - 32 P] radiolabeled probes.

NF- κB: 5'-TCA ACA GAG GGG ACT TTC CGA GAG GCC-3' (115)

AP-1: 5'- CGC TTG ATG ACT CAG CGG GAA-3' (116)

Oct-1: 5'- TGT CGA ATG CAA ATC ACT AGA A-3' (117)

The sequences of [γ - 32 P] radiolabeled probes used to confirm NF-κB binding sites within the promoter of DP103 are:

probe#1: 5'-TCTCCTCCCTCTTGGGGCTTTCCT-3',

probe#2: 5'-AGAGGCGGGGCGGTGCCCCACCG-3' and

probe#3: 5'-CACGGCTGGGCGGCTCCGCCAG-3'.

The DNA probe was radiolabeled by incubation at 37°C for 30min with the following: 5x forwarding buffer, 32 P- γ -ATP and T4 kinase (10unit/ μ l). The labeled probe was then spun at 3000 rpm for 1min to get rid of the buffer, followed by loading into the G50 micro column (Pharmacia Biotech, UK) and spun for 2min for purification. EMSA was performed in a reaction mixture containing 2x reaction buffer (50% glycerol, 1M HEPES pH 7.9, 1M Tris-HCl pH 8.0, 0.5M EDTA pH 8.0, 100mM DTT), 0.5 μ g/ μ l poly (dI-dC), protein samples and 1 μ g/ μ l BSA and kept on ice for 10min before adding DNA probes. The mixture was then kept at room temperature for another 20min before loading into a non-denaturing polyacrylamide gel and run for 1h. The gel was then dried and analyzed with a PharoFX Plus system (BioRad, Hercules, CA).

Gel zymography

Equal serum-free growth media collected from tested samples as indicated were subject to Electrophoresis using 10% denaturing polyacrylamide gels containing 0.1% gelatin. Following electrophoresis, the gels were re-natured with 50mM Tris-HCl buffer (pH 7.5) containing 2.5%

Triton X-100 for 30min, and incubated at 37°C for 16h in a buffer composed of 0.15M NaCl, 10mM CaCl₂ and 50mM Tris-HCl (pH 7.5). The gels were stained with 0.5% Coomassie blue in 5% methanol and 10% acetic acid in dH₂O, and destained with 10% methanol and 5% acetic acid.

Luciferase assay

1.25x10⁵ cells/well was plated in 12-well plates. Experiments were set up as described. The cells were then transfected with luciferase reporter plasmid containing 3x NFκB or AP-1 binding sites together with *Renilla* plasmid (Clontech, Palo Alto, CA). At time of harvest, the promoter activity was assessed with a dual-luciferase assay kit (Promega, Madison, WI). Briefly, feeding medium was removed from the wells, washed once with 1x PBS, and lysed with ice-cold 100μl of reporter lysis buffer. Ten microlitres of cell lysate was then added to 50μl of luciferase substrate solution, following which 50μl of stop & glow buffer was added for *Renilla* reading. Bioluminescence generated was measured using a Sirius luminometer (Berthold Detection System, Pforzheim, Germany). The luminescence readings obtained were normalized to the protein concentration of the corresponding cell lysate and presented as fold difference with reference to the control setup.

Cell viability

MDA-MB-231 cells were plated in 12-well plates. Experiments were set up as described. At the end of drug treatment or transfection, medium was removed from wells. The cells were then washed once with 1x PBS. This was followed by incubation with 0.5ml of crystal violet solution (0.75% crystal violet, 50% ethanol, 1.75% formaldehyde, 0.25% NaCl) for ten minutes. Excess

crystal violet solution was carefully washed away with distilled water for several times and the wells were left to air-dry. The remaining crystals were dissolved in a 1% SDS in 1x PBS solution and its absorbance read at 595nm and converted to percentages, with control setups at 100%.

Mammary fat pad spontaneous metastasis model

Ten-week old female Balb/c nude mice (Animal Resource Centre, Western Australia) were anaesthetized prior to surgery and a 5mm incision was made in the skin to expose the abdominal mammary fat pad (m.f.p.). Two million cells in 0.03ml were injected into the tissue through a 27-gauge needle. Tumor growth was monitored weekly by bioluminescence imaging using the IVIS™ camera system (Xenogen, Alameda, CA, USA). For *ex vivo* imaging, 150mg/kg D-luciferin (Xenogen) was injected into the mice just before necropsy. Tissues of interest were excised, placed into tissue culture dish and imaged for 1min. Regions of interest from displayed images were quantified as photons per second (p/s) using Living Image Software (Xenogen).

2D migrational assays

Glass cylinders (Biopetechs, Butler, PA) of 6mm inner diameter were placed vertically on tissue culture dish. About 20000 cells were seeded inside the glass cylinders and incubated at 37°C in a humidified atmosphere at 5% CO₂ for 24h. The cylinders were then carefully lifted from the dish to reveal an undisturbed circular monolayer patch of cells, which were then washed thrice with 1x PBS to remove dead cell debris and refilled with 2ml of complete medium. Live video monitoring assays of the migrating cells at the edge of the monolayer were performed using phase contrast microscopy (Biostation IM, Nikon). Rectangular fields of view with pixel resolution 1280x960 were chosen from the monolayer edge using the proprietary software and videos were recorded for 24 hours with 10min intervals in between the frames (total 145 frames).

Fifty cells from 6-8 rows of the leading edge of the monolayer were manually tracked using the open source software Image J. Monolayer edge distances (MED) were measured as the average of the displacements (n=5 per field of view measured for 4-5 videos per experiment) between the initial and final positions of the monolayer edge. 2D track plots and plot related measurements were performed using the Chemotaxis tool plugin (Integrated BioDiagnostics).

In vitro and 3D invasion assay

In vitro invasion assay was performed using BD Bio-Coat Matrigel invasion assay system (BD Biosciences, San Jose, CA) according to the manufacturer's instructions. For 3D invasion assay, Nutragen™ collagen solution (Inamed Biomaterials, Fremont, CA, US) was mixed with NaOH, 10x PBS, and MDA-MB-231-GFP cells suspended in serum-free DMEM on ice. The final solution contained 4mg/ml of collagen-I and around 200,000/ml cells. 30-60min incubation under 37°C humidified chamber led to the self-assembly of a piece of semi-spherical cell-seeded collagen gel in the central well of a glass-bottomed dish. Complete cell culture media were immediately supplied to the gel to support cell growth. After 40h, these GFP-expressing cells were imaged in 3D collagen hydrogel using confocal fluorescence microscopy (Nikon TE2000-EZ C1 system). Ten hours of time-lapsed confocal imaging was then carried out in an environment chamber maintaining 37°C and 5% CO₂ atmosphere, which was completed within 70h post siRNA transfection. Quantitative image analysis was achieved using 3D reconstruction and cell tracking function provided by Imaris (Bitplane, Zurich, Switzerland).

GST-IκBα Kinase Assay

MDA-MB-231 cells were transfected with DP103 for overexpression or siDP103 for knock-down. After 36 h, the cells were lysed with IP buffer and the kinase complex was prepared by IP

using anti-NEMO antibody. GST-IκBα/1-66 was purified using glutathione-agarose column (Thermo Sci., MA) and used as the substrate. The reaction was performed with mixture of kinase complex, 0.5μg of GST-IκBα/1-66, and ATP [P^{32}], in kinase buffer (20 mM Hepes (pH 7.7), 2mM MgCl₂, 2mM MnCl₂, 1mM DTT, 10μM ATP + inhibitors (0.5 mM PMSF, 10mM beta-glycerol phosphate (BGP), 300μM sodium othovanadate, 1μg/ml leupeptin, 1μg/ml aprotin, 10mM sodium fluoride, 10mM p-nitrophenyl phosphohate) at 37°C for 1h. The samples were subjected to 12% SDS-PAGE and visualized by autoradiography. The purified IKK complex and GST-IκBα/1-66 were analysed by western blotting with proper antibodies.

Clinical materials

Table S1A – Singapore Cohort

Tissue microarray (TMA) slides consisting of invasive ductal carcinoma (IDC) cases from 399 patients and normal non-malignant ductal tissues from 61 women were obtained from the Department of Pathology, Singapore General Hospital. As a result of tissue loss during immunohistochemical processing, the following number of cases (invasive ductal carcinoma and normal non-malignant ductal tissues) were available for evaluation: DP103 [Proteintech, Chicago, IL, USA (catalogue 11324-1-AP)] (330 and 38 respectively); phospho-p65 (S276) antibody [Abcam, Cambridge, MA, USA (catalogue ab30623)] (338 and 49 respectively); MMP9 [Proteintech, Chicago, IL, USA (catalogue 10375-2-AP)] (357 and 53 respectively). Clinicopathological features were recorded for statistical analyses, including age of patient, ethnic group, tumor type, and histological grade of tumor. Patient survival and tumor recurrence data were available for 329 cancer patients. The period of follow-up ranged from 0 to 156 months. Deaths (defined as being resultant from the cancer itself) occurred in 21.1% of patients, with the mean and median overall survival (OS) periods being 112 and 117 months respectively.

Among patients with tumor recurrence, 20.1% of them were dead at the end of the study period, with a mean survival after recurrence (SAR) period of 17 months and median SAR of 0 month. OS was defined as the time from diagnosis to death. SAR was defined as the survival duration from the first recurrence to death. Cases that did not reach the defined end-points of interest were censored at the date of last follow-up.

Table S1D – Canada Cohort

This study was performed on 190 archived formalin fixed paraffin embedded (FFPE) blocks containing tissues obtained from female patients. All samples were obtained from Centre hospitalier de l'Université de Montréal (CHUM). The collected blocks contain both invasive and in situ carcinoma of breast and normal breast tissue from healthy women undergoing plastic surgery.

Table S3A – China Cohort

A cohort of a total of 63 primary breast cancer and 22 benign breast tissue samples derived from 85 patients who underwent surgery at the First Affiliated Hospital of Anhui Medical University (Hefei, Anhui, People's Republic of China) between 2009 and 2010 was obtained. All tissue samples were hematoxylin and eosin stained and had been reviewed by two independent pathologists in Anhui Medical University. Total RNA from these breast tumor tissue samples was extracted by TRIzol® (Invitrogen, Life Technologies, Grand Island, NY), reversely transcribed into cDNA by using RevertAid First Strand cDNA Synthesis Kit (K1622, Fermentas, Germany) and Real-time PCR was carried out by using SYBR Premix Ex Taq (DRR041A, TaKaRa, Shiga, Japan) in a Stratagene MX3000P detection system (Stratagene, La Jolla, CA, USA). The amplification protocol was set as following: an initial 95°C for 5min and then 40 cycles of denaturation at 95°C for 5sec, annealing and extension at 60°C for 30sec. Primer sequences used for qPCR expression in patient tissues from First Affiliated Hospital of Anhui Medical University

are DP103-F: 5'-TGCCAGTAAACAGATGC-3', DP103-R: 5'-GTGCCAAAGGGTATGA-3';
MMP9-F: 5'-CGAACTTTGACAGCGACAAGA-3', MMP9-R: 5'-
AGGGCGAGGACCATAGAGG-3'; GAPDH-F: 5'-TGCACCACCAACTGCTTAGC-3',
GAPDH-R: 5'-GGCATGGACTGTGGTCATGAG-3'; HMGB1-F: 5'
TTGTCTGGGAGGAGCATAA 3', HMGB1-R: 5' GGGCGATACTCAGAGCAGAA 3';
H2AFZ-F: 5' CAAGACAAAGGCGGTTTC 3', H2AFZ-R: 5' GCATTTCTGCCAGTTCA 3'.

Immunohistochemistry

DP103, MMP9, and phospho-p65 (S276) antibodies were used for immunohistochemical staining of the TMA sections. Briefly, the TMA sections were deparaffinized in Clearene and rehydrated through a graded series of ethanol. Endogenous peroxidase activity was quenched with 3% hydrogen peroxide for 30 min. Antigen retrieval was carried out through heating in 10mM citrate buffer (pH 6.0) at 90-100°C for 20 min. The sections were blocked with goat serum for 1hr prior to overnight incubation at 4°C with the primary antibody (1:50 dilution). The staining pattern was visualized using the Dako Envision-HRP kit with diaminobenzidine as the substrate. Sections were counterstained using Shandon's hematoxylin.

Immunohistochemical evaluations

The intensity of the staining in the epithelial compartment of ductal tissues was noted as absent (0), weak (1+), moderate (2+), or strong (3+). Low expression of DP103, phospho-p65 and MMP9 was defined as staining intensity of 0 or 1+, whereas high expression denotes staining intensities of 2+ or 3+. Evaluation of the stained TMA sections was carried out by two independent blinded observers, including a trained histopathologist.

SUPPLEMENTARY FIGURE LEGENDS

Figure S1. DP103 staining in (A) a normal ductal tissue and (B) an invasive ductal carcinoma. (C) The gene expression value of DP103 (y-axis) is plotted for each breast cancer subtype. DP103 staining in (D) a normal ductal tissue, (E) in a Luminal A subtype, (F) in a Luminal B subtype, (G) in a HER2 subtype and (H) in a Basal subtype from cohort in Table S1A. DP103 staining in (I) a normal ductal tissue, (J) in a Luminal A subtype, (K) in a Luminal B subtype, (L) in a HER2 subtype and (M) in a Basal subtype from cohort in Table S1B. (N) Box and whisker plots of DP103 expression level distributions in tumors defined by histologic grade (Nottingham grading system). Shaded rectangles represent interquartile range; central line represents median value.

Figure S2. DP103 staining (A) in normal non-malignant ductal tissue, (B) in low grade invasive ductal carcinoma, (C) in invasive ductal carcinoma of tumor grade 2 and 3 and (D) in high grade invasive ductal carcinoma from cohort in Table S1A. Cell nuclei were counterstained with haematoxylin. DP103 staining in (E) in grade I invasive ductal carcinoma, (F) in invasive ductal carcinoma of grade II tumor and (G) in grade III invasive ductal carcinoma from cohort in Table S1B. DP103 mRNA expression positively correlates to expression of metastasis genes (H) HMGB1 and (I) H2AFZ in 85 human breast patients from cohort in Table S1C showing positive correlation using Pearson's Correlation Coefficient.

Figure S3. (A) Transfection efficiencies of the two different siRNAs and in combination on expression of DP103 in MDA-MB-231 and BT549 cells. (B) MDA-MB-231 cells were subjected to siRNA knockdown of DP103 and the monolayer edge distances of the cells were tracked using

live microscopy. (C) 2D plots of individual cell migration tracks with starting point of all the cell tracks coincided at the origin. Top and bottom left: control siRNA (ctsi) treated MDA-MB-231 show increased migratory distances with 72% of cells outside a radius of $101\mu\text{m}$ that coincides with the centre of mass (positive sign) of all the cell coordinates. Top and bottom right: siRNA against DP103 treated MDA-MB-231 show decreased migratory distances with 46% cell inside a radius of $74\mu\text{m}$ that coincides with the centre of mass of all the cell coordinates, and 56% of cells inside a radius of $101\mu\text{m}$ in comparison to ctsi. X and Y axes represent migration distance in μm . (D) Analyses of cell migration tracks. ctsi show a significant increase in the Accumulated distance (top left), Euclidean distance (top right), mean cell speed (bottom left) and confinement ratios (bottom right) in comparison to siDP103 cells. Box edges represent standard deviation; the small square within the box represents the mean and divider at 50% value.

Figure S4. (A) Cell displacement (μm) tracks in 3D collagen gel. The tracks of a population of cells ($n>50$) were adjusted to start from the same origin (0,0,0). (B) The histogram of cells speed averaged over each track, track number >50 . The height of each column corresponds to the percentage of tracks of a certain speed. (C) 3D Z-stack of confocal images was projected to X-Y plane, and cell morphology was shown with fluorescence from GFP. Left: Cells transfected with control siRNA (ctsi); Right: DP103 knockdown cells. Loss of pseudopodial protrusions in cells after siDP103 (white arrows). (D) MDA-MB-231 cells were transfected with pcDNA3/EV and pcDNA3-FLAG-DP103 (DP103/F-DP103). Cells extract immunoblotted with anti-DP103 antibodies. (E) MDA-MB-231 cells were transfected as stated in D and prepared for invasion assay. (F) MDA-MB-231 cells that invaded through the chambers counted and represented in percentages * denotes $p<0.05$.

Figure S5. (A-B) Different expression levels of MMP9 between (A) normal ductal tissue and (B) invasive ductal carcinoma tissue. (C) DP103 and MMP-9 mRNA expression levels in 85 human breast patients were determined and showed positive correlation using Pearson's Correlation Coefficient ($r^2=0.5686$). (D) DP103 mRNA expression levels correlates positively with MMP9 mRNA expression in basal and claudin-low subtypes. (E) Pearson's Correlation Coefficient was determined between the mRNA expression of DP103 and MMP9 in various breast cell lines. DP103 knockdown in another invasive breast cancer cell line, HS578t, showed drop in (F) mRNA levels of MMP9 and (G) MMP9 protein levels * denotes $p<0.05$. (H) MDA-MB-231 and (I) BT549 cells transfected with either control siRNA or siDP103. Cell viability determined by crystal violet assay.

Figure S6. (A) MDA-MB-231 and MCF10A cells were transfected with pcDNA3 (EV) and pcDNA3-FLAG-DP103 (DP103). Cells extract immunoblotted with anti-DP103 and anti-MMP-9 antibodies. (B) MDA-MB-231 cells assayed for invasion capability with either MMP2/9 inhibitor (SB-3CT, 10 μ M) or pan-MMPs inhibitor (GM6001, 50 μ M) (10X magnification). Insert shows zoomed pictures (40X magnification). (C) The number of cells invaded through the transwell invasion chambers from (B) counted and represented * denotes $p<0.05$. (D) MDA-MB-231 cells transfected with either empty vector (pcDNA3) or DP103 (DP103) assayed for transwell invasion with or without MMP9 Inhibitor I (1 μ M). The number of cells that invaded through the transwell invasion chambers counted and represented * denotes $p<0.05$.

Figure S7. Control siRNA and siDP103 treated BT549 cells transfected with *Renilla* and luciferase reporter plasmid containing NF κ B. The cells were subsequently stimulated with (A) 10 μ M VP16, (B) 25 μ M doxorubicin and (C) 10 μ M CPT for 0h, 6h, and 12h and then harvested

for luciferase assay. Results are expressed in fold difference and are the average of three separate experiments * denotes $p < 0.05$. Control siRNA and siDP103 treated BT549 cells were transfected with *Renilla* and luciferase reporter plasmid containing AP-1. The cells were subsequently stimulated with (D) 10 μ M VP16, (E) 25 μ M doxorubicin and (F) 10 μ M CPT for 0h, 6h, and 12h and then harvested for luciferase assay. Results are expressed in fold difference and are the average of three separate experiments * denotes $p < 0.05$. (G) MDA-MB-231 cells transfected with control siRNA or siDP103. Cells were left untreated or treated with CPT (10 μ M) for indicated times. Protein extracts were examined with (top) EMSA and (bottom) Western blotting of nuclear and cytoplasmic protein fractions using antibody human-anti-p65, human-anti-DP103 and human-anti-GAPDH. (H) MDA-MB-231 cells were transfected with either control siRNA or DP103 siRNA and treated with or without (H) 10 μ M CPT or (I) 25 μ M doxorubicin for 48h. Graph showing percentage of cell viability (bottom) from three separate experiments * denotes $p < 0.05$. (J) MDA-MB-231 cells transfected with control siRNA or siDP103. Cells were either left untreated or treated with CPT as indicated. Protein extracts were examined with EMSA and Western blotting using human-anti-DP103 and human-anti-GAPDH antibodies.

Figure S8. (A) Map showing the FLAG-tagged wild-type (WT) and GNT mutant with single amino acid mutated in the helicase domain of DP103. (B) MDA-MB-231 cells transfected with either empty vector (EV), wild-type DP103 (WT) or GNT mutant (GNT) and assayed in transwell invasion chamber for 48h. Insert shows zoomed pictures. (C) The number of cells that invaded through the transwell invasion chambers in (B) counted and represented * denotes $p < 0.05$. (D) MDA-MB-231 cells transfected with pGNT mutant were stimulated with TNF α for 10min. 0.5mg of protein lysate were immunoprecipitated with TAK1 and IgG antibodies and IP

material and lysates were analysed by immunoblotting with the indicated antibodies. Western blot analysis of the input lysate is shown in the panel below.

Figure S9. (A) MDA-MB-231 cells were stimulated with TNF α for 10min. 0.5mg of protein lysate were immunoprecipitated with TAB2 and IgG antibodies and IP material and lysates were analysed by immunoblotting with the indicated antibodies. (B) MDA-MB-231 cells were stimulated with TNF α for 10min. 0.5mg of protein lysate were immunoprecipitated with TAB3 and IgG antibodies and IP material and lysates were analysed by immunoblotting with the indicated antibodies. (C) Purified recombinant full-length GST-TAK1 and His-DP103 proteins were stained using Coomassie blue staining. (D) Coomassie blue staining of purified GST-IKK2-WT and GST-IKK2-Mut proteins. The sequences are shown in the bottom panel and the amino acids in red indicate the wild type and mutant TAK1 phosphorylation sites in the activation loop of IKK2. (E) MDA-MB-231 cells transfected with siRNA control or siRNA against DP103 were stimulated with TNF α for 10min. 0.5mg of protein lysate were immunoprecipitated with TAK1 and IgG antibodies and IP material and lysates were analysed by immunoblotting with the indicated antibodies. Western blot analysis of the input lysate is shown in the panel below. (F) MDA-MB-231 cells infected with empty vector (EV) or pBOBI-DP103 were stimulated with TNF α for 10min. IP material and lysates were analysed by immunoblotting with the indicated antibodies as described in (E).

SUPPLEMENTAL TABLES

Table S1. (A) Clinicopathological features of number of cases from Singapore cohort. Collated expression analysis of DP103 epitope in the epithelial compartments of indicated number of

ductal specimens from (B) Singapore cohort and (C) Canada cohort. (D) Clinicopathological features of number of cases from Canada cohort.

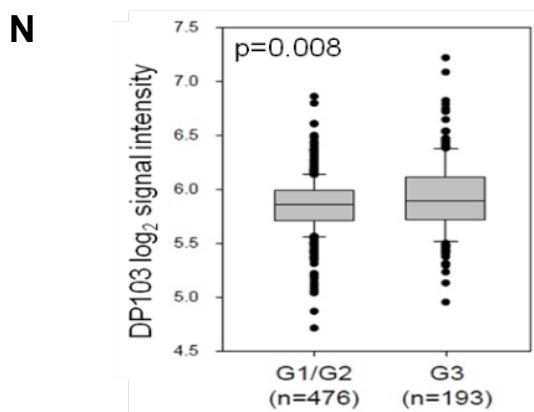
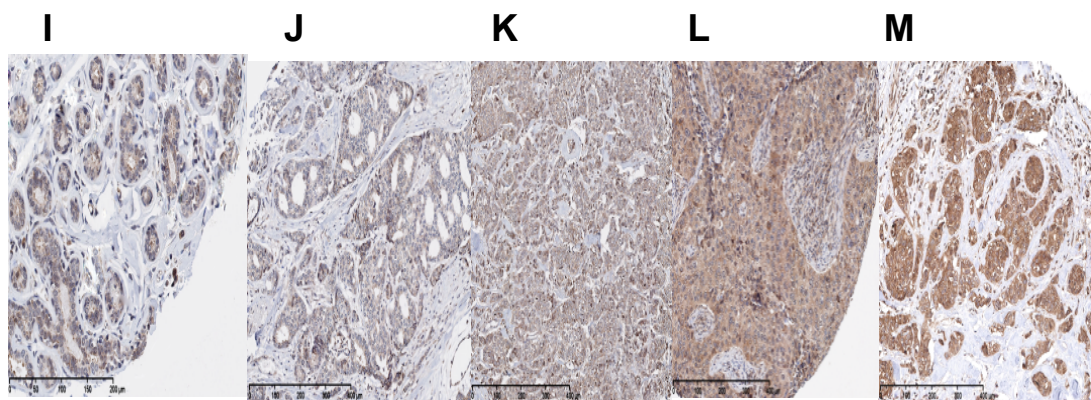
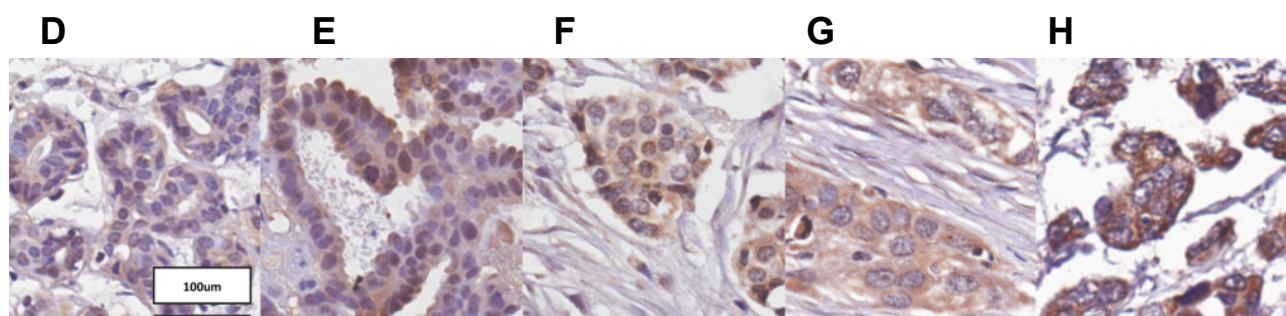
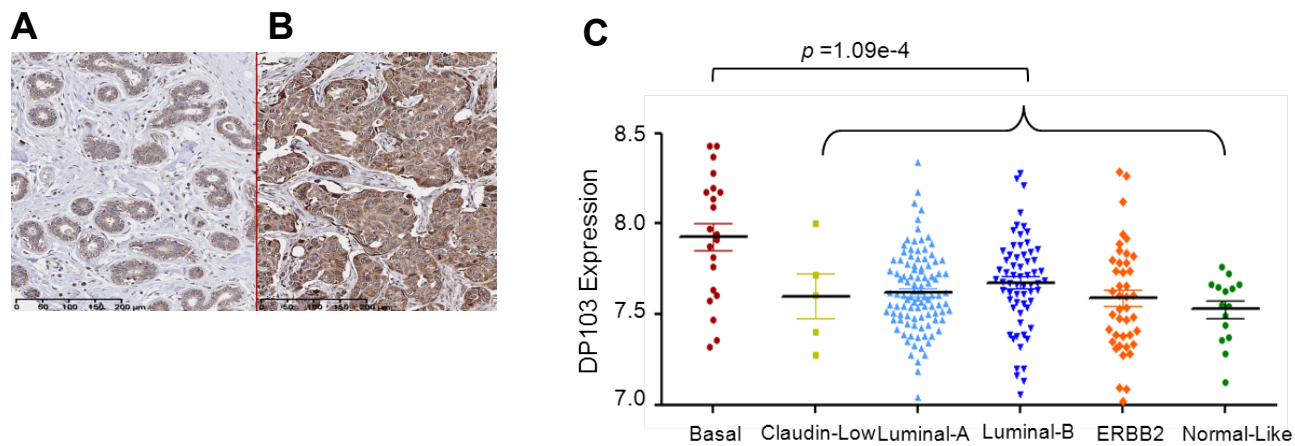
Table S2. Collated expression analysis of DP103 epitope in basal and non-basal breast tumor subtypes in specimens from (A) Singapore cohort and (B) Canada cohort. Association analyses on expression of DP103 in the various tumor grades were determined using Fisher's Exact and Kendall-Tau tests in specimens from (C) Singapore cohort and (D) Canada cohort. Analysis of the tissue microarrays showed that the staining intensity of DP103 in the epithelial compartment was highly significantly associated with histological tumor grade.

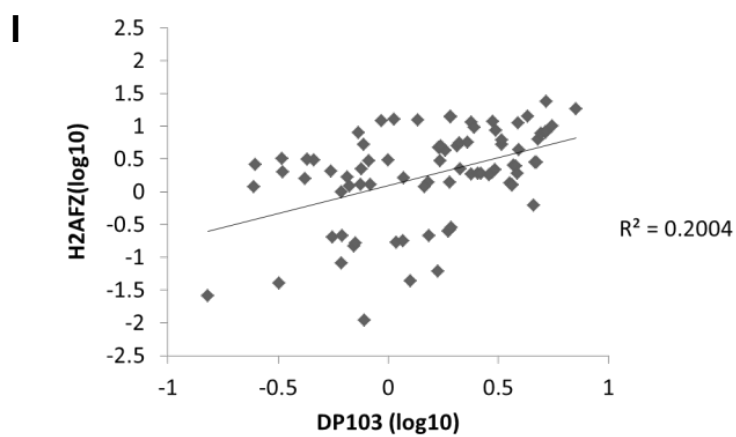
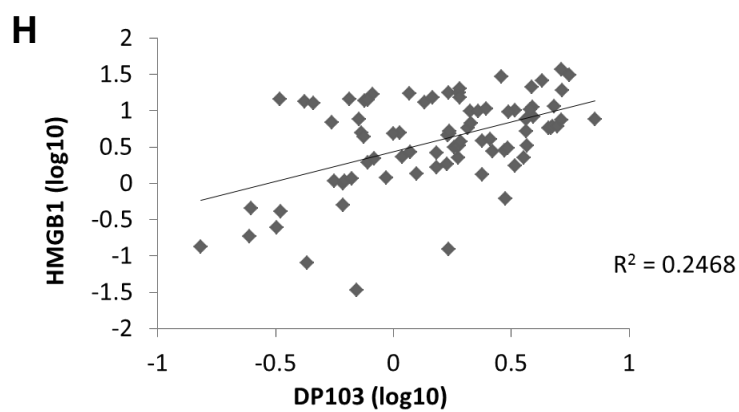
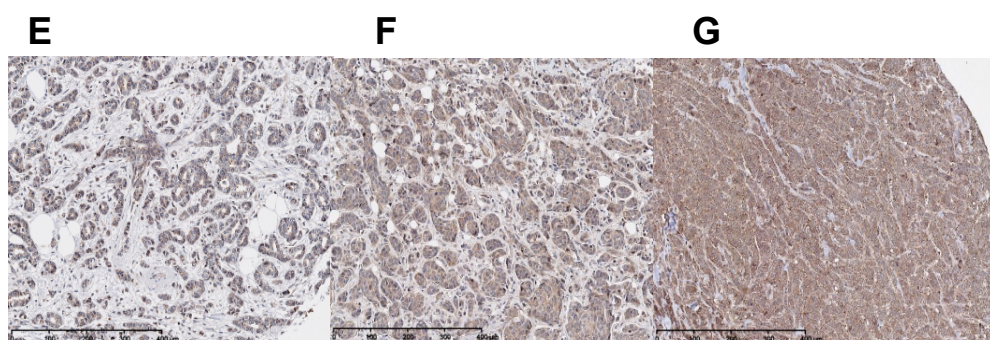
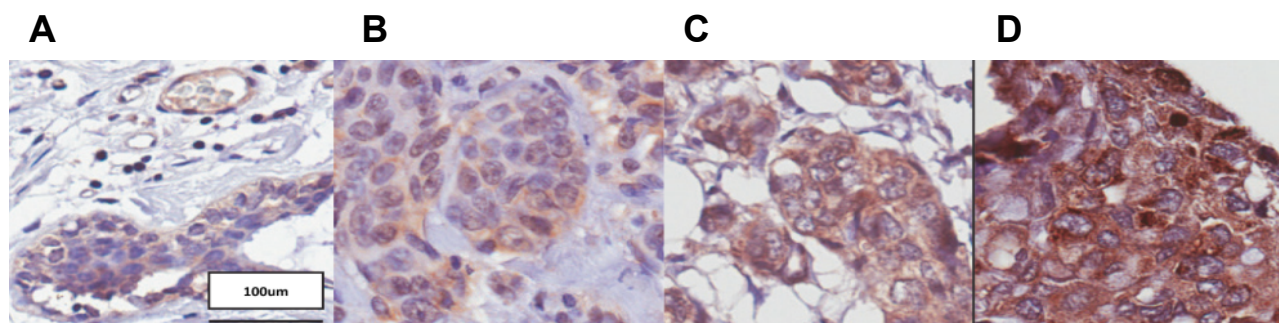
Table S3. (A) Clinicopathological features of number of cases from China cohort. (B) Spontaneous metastases from orthotopic mammary fat pad implant. Two million cells empty vector transfected MDA-MB-231 cells (MDA-MB-231-EV) or DP103 transfected cells (MDA-MB-231-DP103) are injected orthotopically into the abdominal m.f.p. of female nude mice. The incidence of pulmonary and liver metastases at necropsy from primary tumors formed by these two cancer cell lines was evaluated by bioluminescence imaging as described in methods and tabulated.

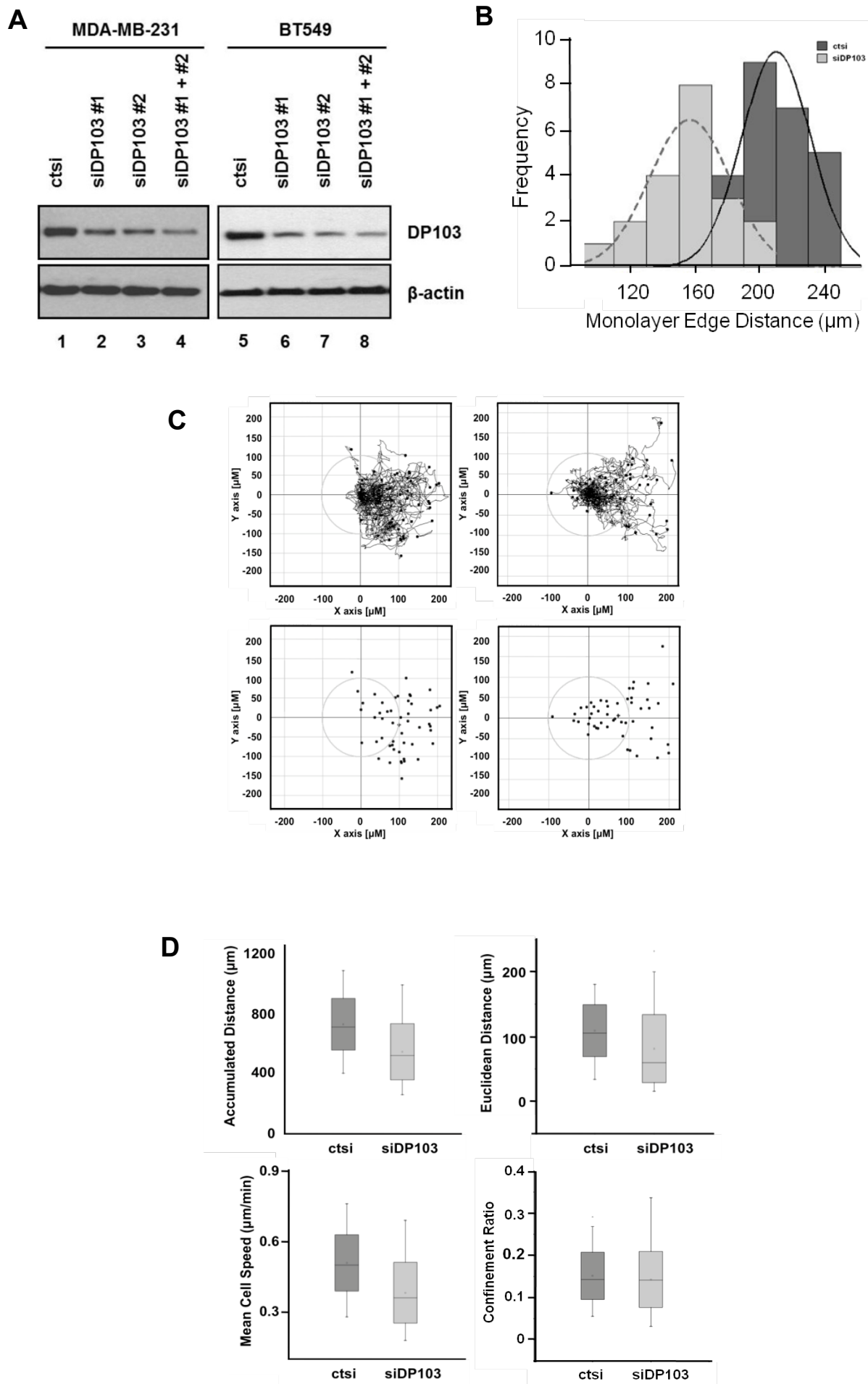
Table S4. Collated expression pattern analysis of MMP9 epitope in epithelial compartments of ductal specimens from (A) Singapore cohort and (B) Canada cohort. Normal non-malignant ductal tissues had reduced staining in comparison to the malignant invasive ductal carcinoma tissues. Association analysis between expression of DP103 and MMP9 were determined using Fisher's Exact and Kendall-Tau tests in specimens from (C) Singapore cohort and (D) Canada

cohort. Results suggested that high DP103 expression is highly significantly correlated with high MMP9 levels.

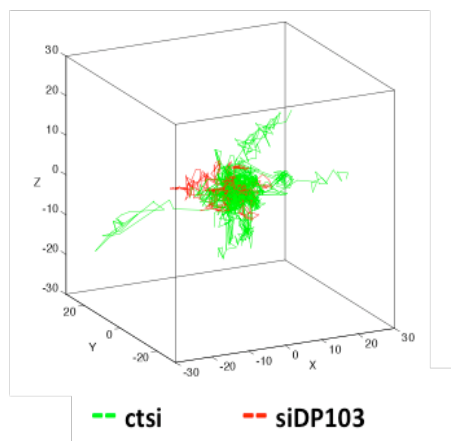
Table S5. (A) Collated expression analysis of phospho-p65 S276 epitope in the epithelial compartments of ductal specimens. Normal non-malignant ductal tissues had reduced staining in comparison to the malignant invasive ductal carcinoma tissues. (B) Collated expression analysis of phospho-p65 S276 epitope and its association with tumor subtype. High expression of phospho-p65 S276 was significantly associated with basal breast tumor subtype. (C) Collated expression analysis of phospho-p65 S276 epitope and its association with histological tumor grades. Analysis of the tissue microarrays showed that the staining intensity of phospho-p65 in the epithelial compartment was highly significantly associated with histological tumor grade. (D) Association analysis between expression of DP103 and phospho-p65 (Ser276) were determined using Fisher's Exact and Kendall-Tau tests. Results suggest that high DP103 expression is highly significantly correlated with high phospho-p65 levels.



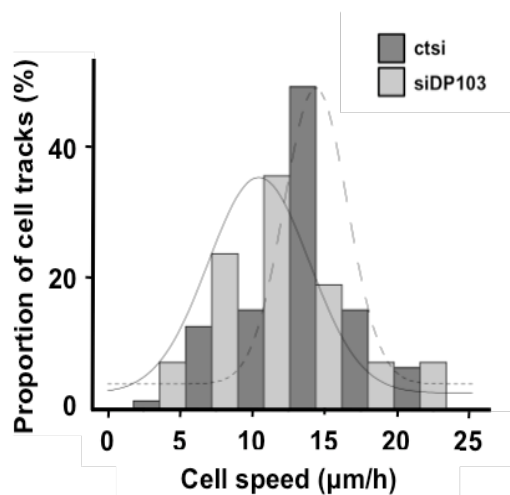




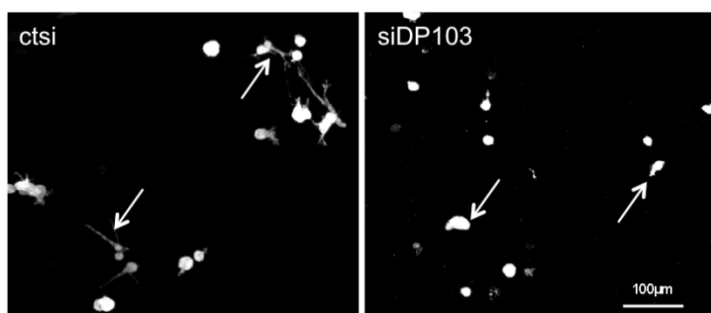
A



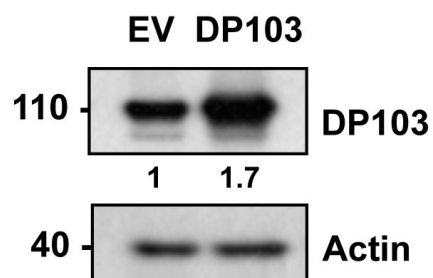
B



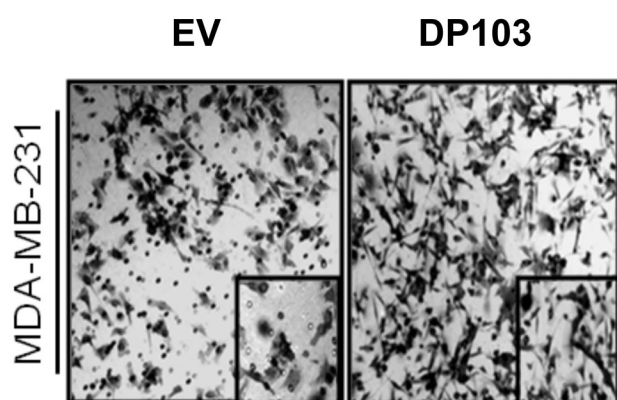
C



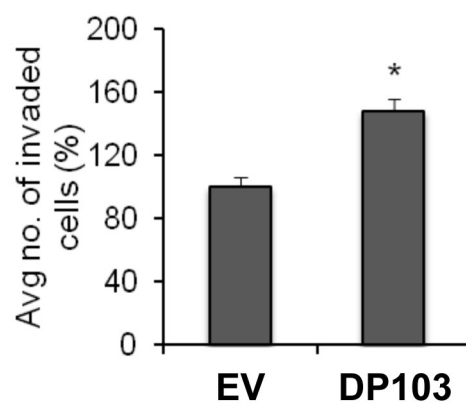
D

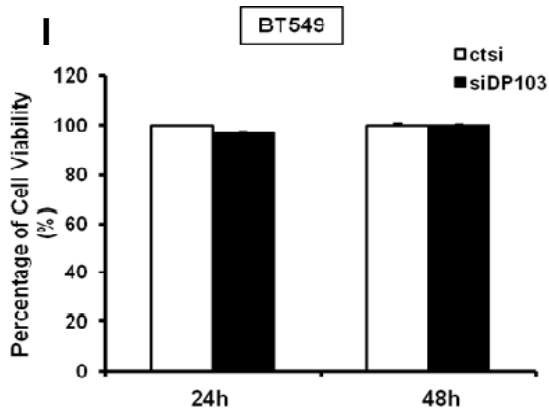
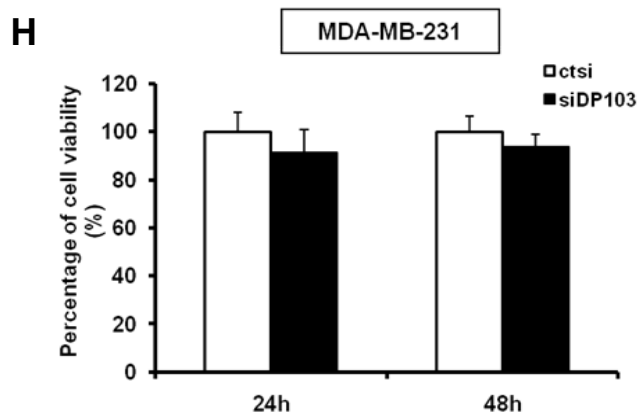
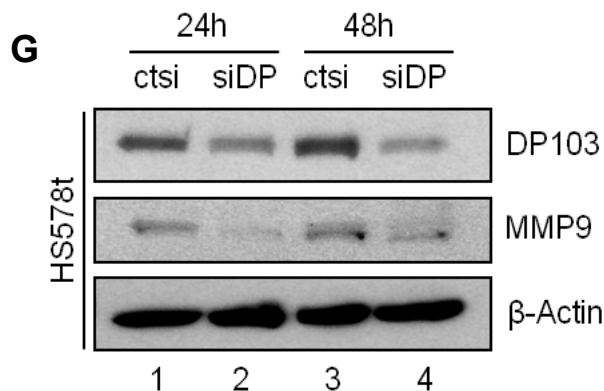
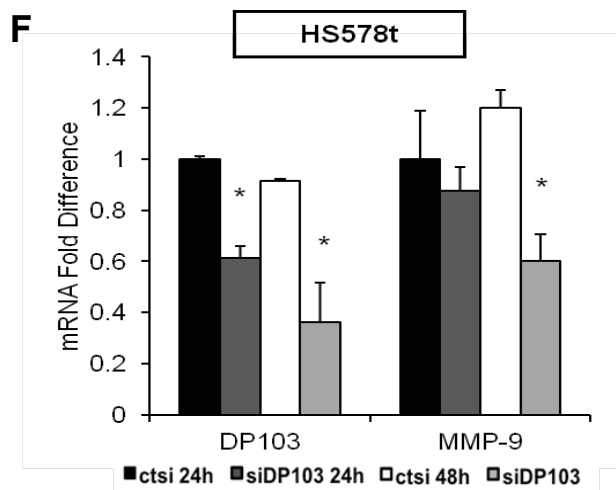
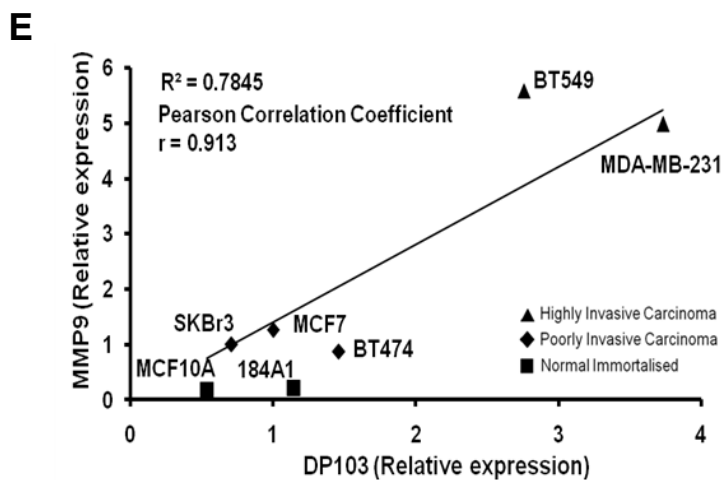
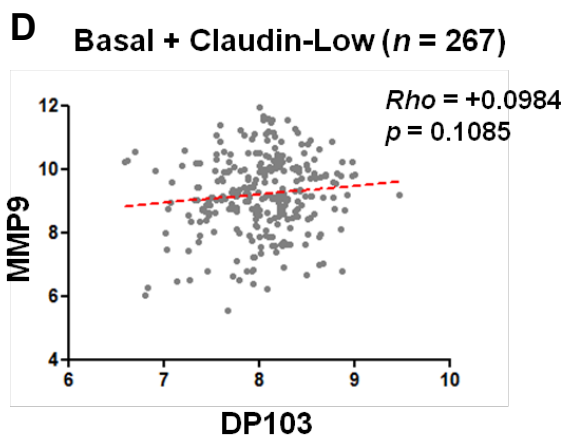
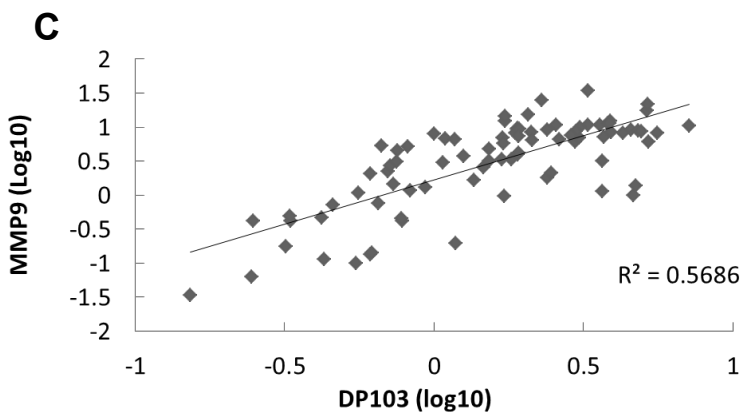
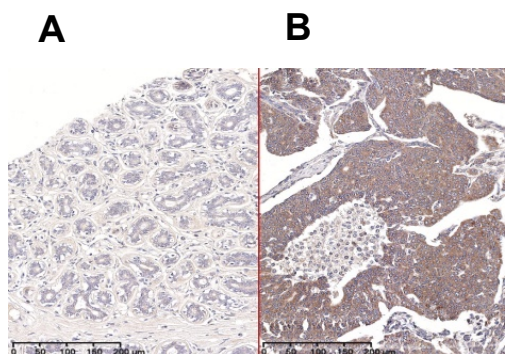


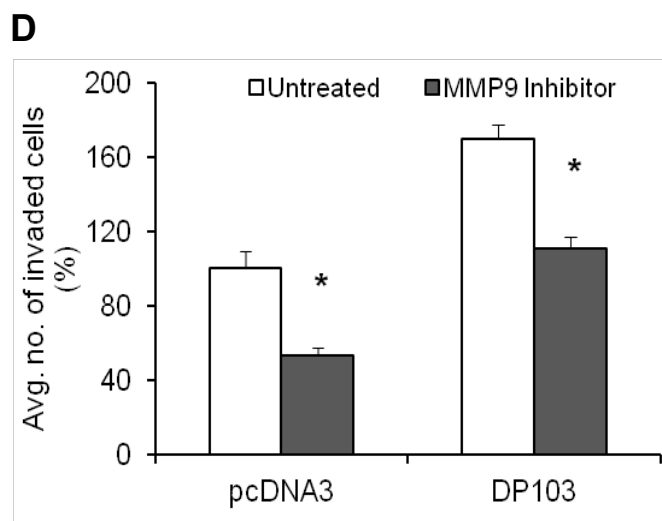
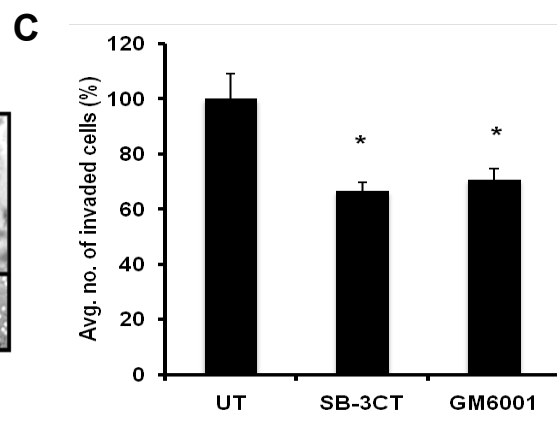
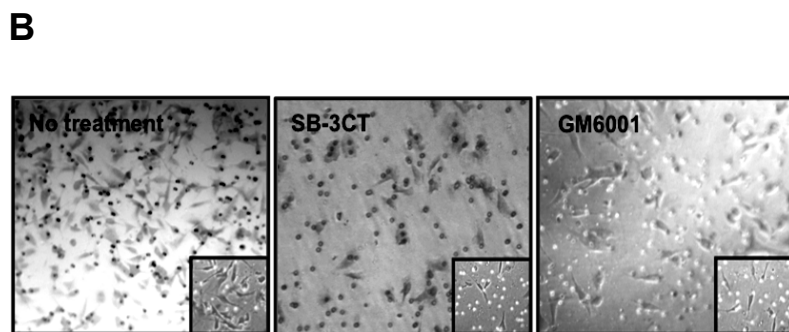
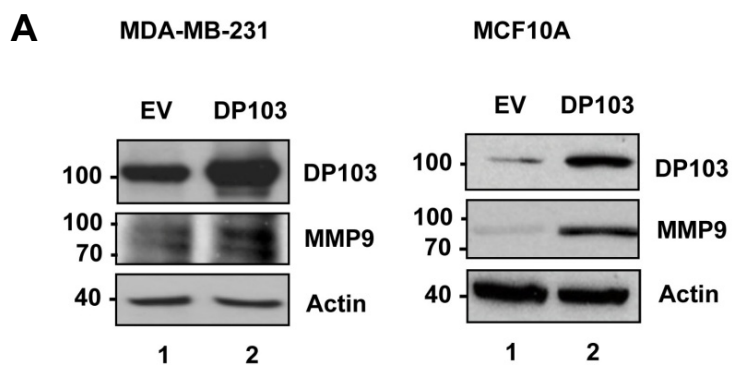
E

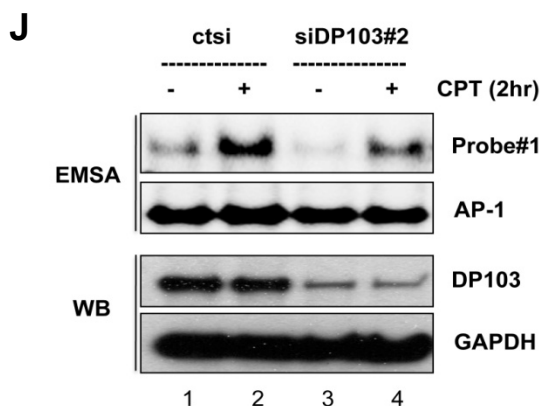
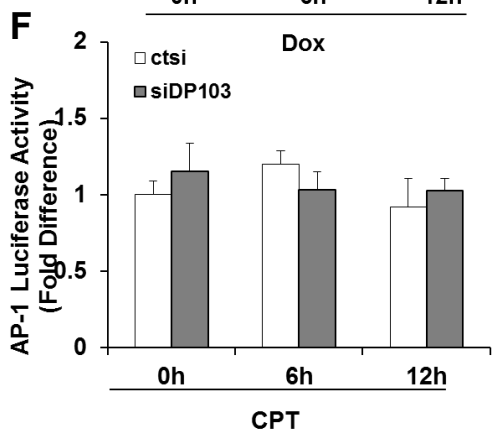
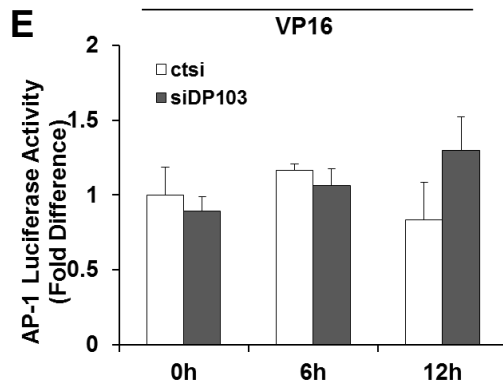
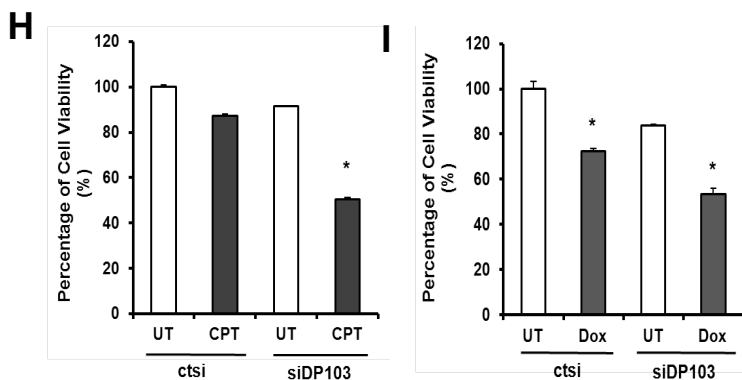
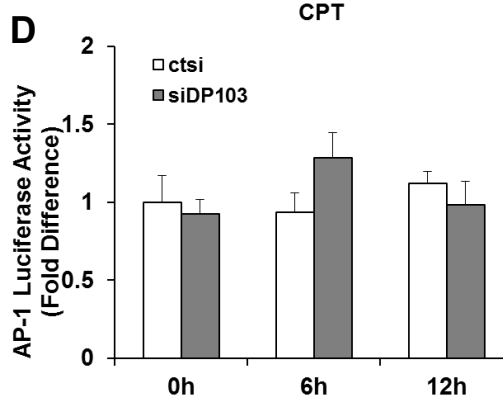
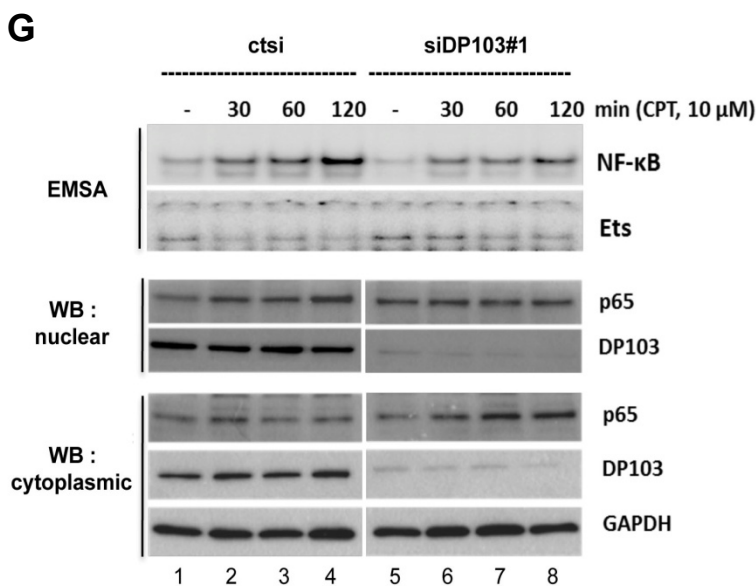
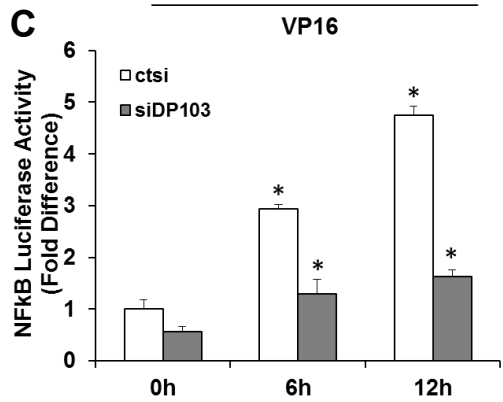
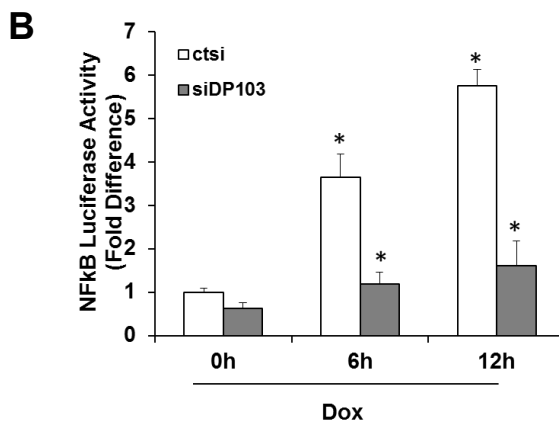
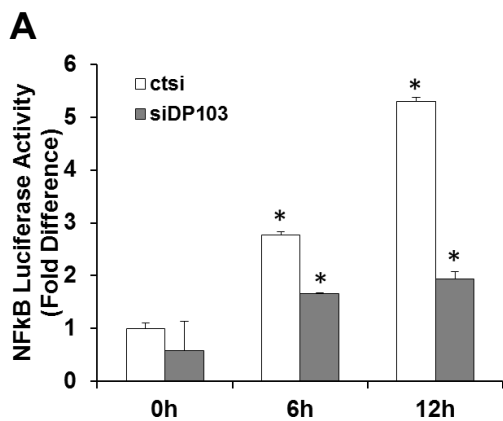


F

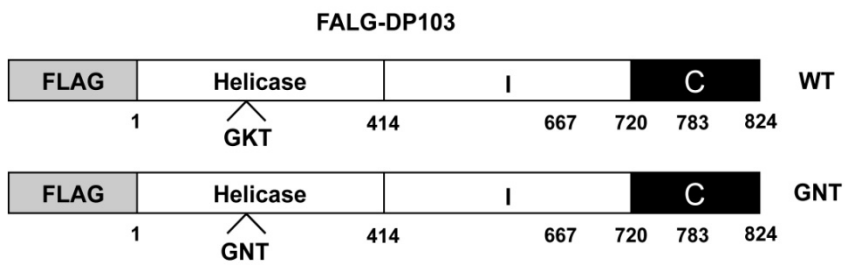




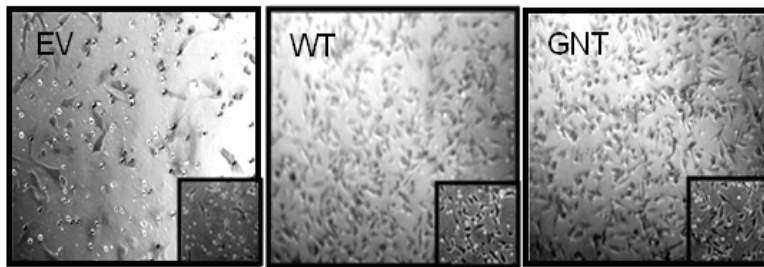




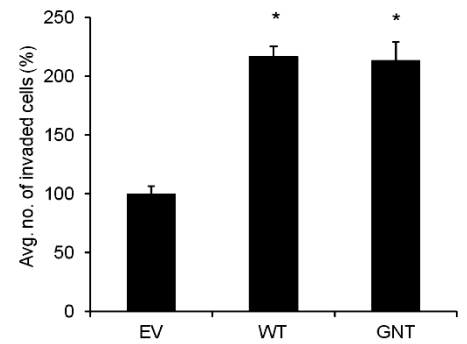
A



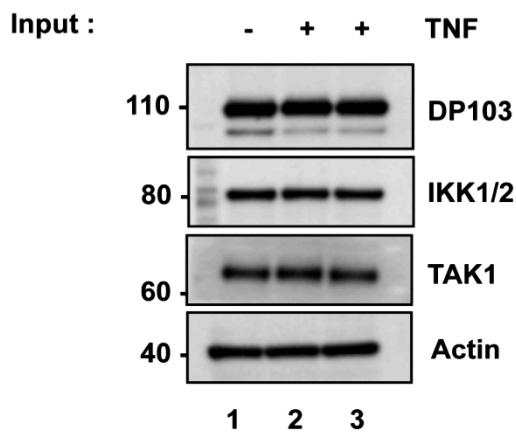
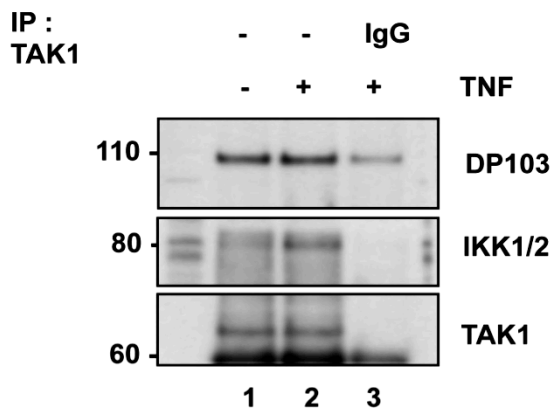
B



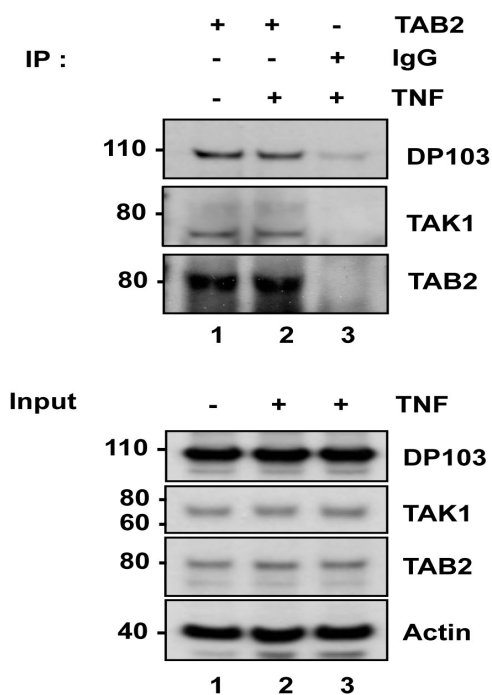
C



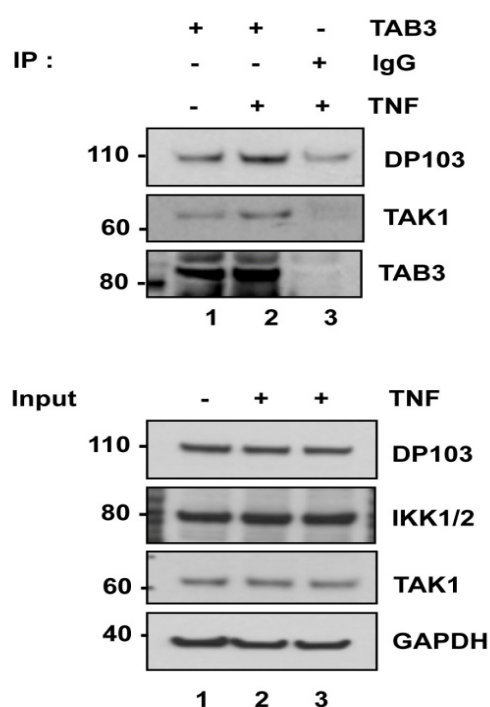
D



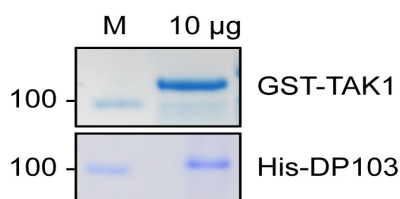
A



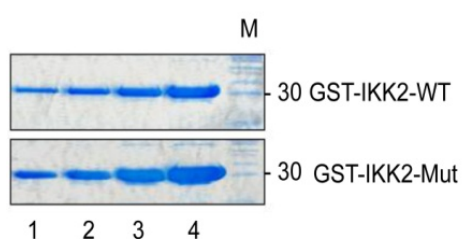
B



C



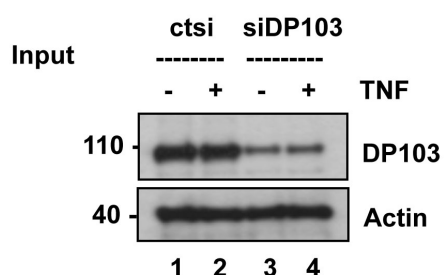
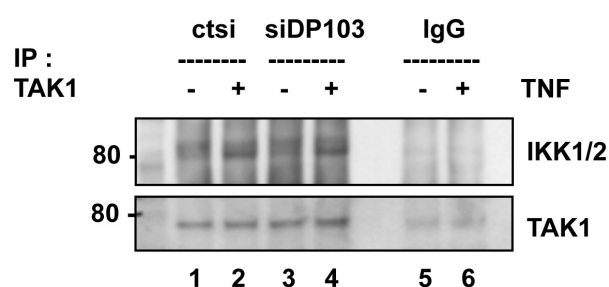
D



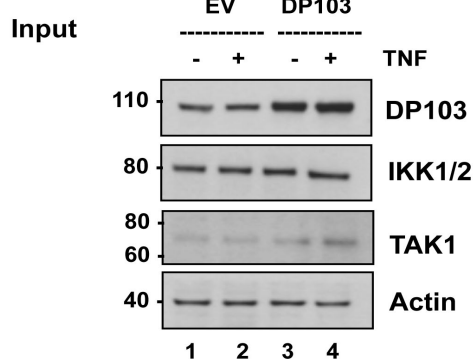
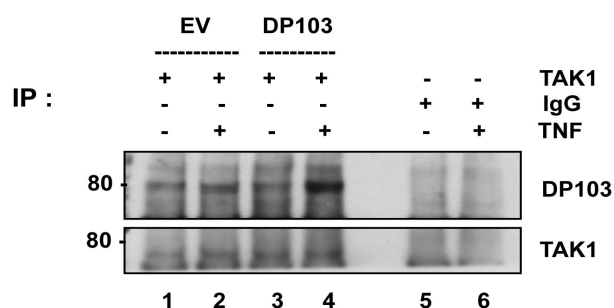
GST-IKK2 amino acid residues (152-204)

GST-IKK2-WT : VLQQGEQRLIHKIIDLGYAKELDQGS**L**CT**S**FVGTGLQYLAPELLEQQKYTVTVD
 GST-IKK2-Mut : VLQQGEQRLIHKIIDLGYAKELDQ**G**AL**C**T**A**FVGTGLQYLAPELLEQQKYTVTVD

E



F



A

Clinicopathological features (Singapore)

Clinicopathological features	Number of cases	Clinicopathological features	Number of cases
Age (years)		Histological tumor grade	
Mean	53	1	66
Median	51	2	151
Minimum	19	3	170
Maximum	86	NA	12
Ethnicity		Tumor type	
Chinese	336	Luminal A	175
Malay	35	Luminal B	38
Indian	17	Basal	60
Others	11	HER2	46
		NA	80

NA = Not Available

B**Clinicopathological features (Canada)**

Clinicopathological features	Number of cases
Age (35-92 years)	411
Grade	
I	38
II	70
III	303
Histological subtypes	
Invasive ductal carcinoma	326
Invasive lobular carcinoma	10
Typical medullary carcinoma	49
Typical medullary carcinoma	19
Colloid carcinoma	7
Estrogen receptors	
Positive	94
Negative	225
Progestron receptors	
Positive	94
Negative	225
HER-2	
Positive	63
Negative	256

C

Clinicopathological features (China)

Clinicopathological features	Number of cases
Age (years)	
= 35	5
35-55	42
> 55	16
Tumor size (cm)	
= 2	26
2-5	34
> 5	3
Lymph node metastasis	
absent	33
present	30
Grade	
I	14
II	37
III	12
Histology	
Ductual	60
Lobular	1
Others	2
Estrogen receptor	
—	19
+	44
Progesterone receptor	
—	22
+	41
c-erbB-2	
low	30
high	33
Ki67	
+	43
++	16
+++	2
++++	2

A

	DP103 expression		
	Low	High	p-value
Diagnosis			
Normal	38	0	<0.001
Malignant	63	267	

B

	DP103 expression		
	Low	High	p-value
Basal	3	47	0.0053
Other tumor subtypes	50	164	

C

	DP103 expression		
	Low	High	p-value
Histological tumor grade			
Normal	38	0	<0.001
1	51	5	
2	5	128	
3	0	133	

D

	DP103 expression		
	Low	High	p-value
Diagnosis			
Normal	15	0	<0.001
Malignant	0	385	

E

	DP103 expression		p-value
	Low	High	
Triple negative	8	144	0.000
Other tumor subtypes	24	157	

F

	DP103 expression		
	Low	High	p-value
Normal	15	0	<0.001
Grade I	2	24	
Grade II	0	47	
Grade III	27	242	

Cell line	No. of mouse with metastasis	Metastasis (p/s)	
		Lung	Liver
MDA-MB-231-DP103	4/11	7.9×10^7	5.4×10^7
		1.0×10^6	8.2×10^7
		1.3×10^6	7.0×10^6
		3.8×10^6	1.3×10^8
MDA-MB-231-EV	1/12	1.9×10^7	2.3×10^7

A

	MMP9 expression		
	Low	High	p-value
Diagnosis			
Normal	53	0	<0.001
Malignant	71	286	

B

	MMP9 expression		
	Low	High	p-value
Diagnosis			
Normal	15	0	<0.001
Malignant	46	339	

C

	DP103 expression		
	Low	High	p-value
MMP9 expression			
Low	56	10	<0.001
High	6	253	

D

	DP103 expression		
	Low	High	p-value
MMP9 expression			
Low	4	74	<0.001
High	19	196	

A

	phospho-p65 expression		
	Low	High	p-value
Diagnosis			
Normal	49	0	<0.001
Malignant	69	269	

B

	phospho-p65 expression		
	Low	High	p-value
Basal	5	47	0.0141
Other tumor subtypes	50	141	

C

	phospho-p65 expression		
	Low	High	p-value
Histological tumor grade			
Normal	49	0	<0.001
1	54	4	
2	4	130	
3	4	134	

D

	DP103 expression		
	Low	High	p-value
Phospho-p65 expression			
Low	55	10	<0.001
High	7	246	